O_2 versus N_2O respiration in a continuous microbial enrichment

Conthe, Monica; Parchen, Camiel; Stouten, Gerben; Kleerebezem, Robbert; van Loosdrecht, Mark C.M.

DOI
10.1007/s00253-018-9247-3

Publication date
2018

Document Version
Final published version

Published in
Applied Microbiology and Biotechnology

Applied Microbiology and Biotechnology
https://doi.org/10.1007/s00253-018-9247-3

ENVIRONMENTAL BIOTECHNOLOGY

O_2 versus N_2O respiration in a continuous microbial enrichment

Monica Conthe[1] · Camiel Parchen[1] · Gerben Stouten[1] · Robbert Kleerebezem[1] · Mark C. M. van Loosdrecht[1]

Received: 14 April 2018 / Revised: 13 July 2018 / Accepted: 15 July 2018

Abstract

Despite its ecological importance, essential aspects of microbial N_2O reduction—such as the effect of O_2 availability on the N_2O sink capacity of a community—remain unclear. We studied N_2O vs. aerobic respiration in a chemostat culture to explore (i) the extent to which simultaneous respiration of N_2O and O_2 can occur, (ii) the mechanism governing the competition for N_2O and O_2, and (iii) how the N_2O-reducing capacity of a community is affected by dynamic oxic/anoxic shifts such as those that may occur during nitrogen removal in wastewater treatment systems. Despite its prolonged growth and enrichment with N_2O as the sole electron acceptor, the culture readily switched to aerobic respiration upon exposure to O_2. When supplied simultaneously, N_2O reduction to N_2 was only detected when the O_2 concentration was limiting the respiration rate. The biomass yields per electron accepted during growth on N_2O are in agreement with our current knowledge of electron transport chain biochemistry in model denitrifiers like *Paracoccus denitrificans*. The culture's affinity constant (K_S) for O_2 was found to be two orders of magnitude lower than the value for N_2O, explaining the preferential use of O_2 over N_2O under most environmentally relevant conditions.

Keywords Nitrous oxide · Mixotrophy · Enrichment · Chemostat

Introduction

Coping with rising levels of the potent greenhouse gas nitrous oxide (N_2O) in the atmosphere calls for the development of mitigation strategies to reduce N_2O accumulation and emission in soil management and wastewater treatment (WWT). The presence and activity of N_2O-reducing organisms in fertilized soils and WWT plants, such as bacteria and archaea harboring *nosZ*-type genes, may be key in such mitigating strategies (Thomson et al. 2012). Nitrous oxide reductase (N_2OR), the enzyme encoded by the *nosZ* gene, is a terminal reductase present in some microbial respiratory electron transport chains (ETC) that catalyzes the only microbial reaction known to consume N_2O, converting it to innocuous N_2 (which constitutes 79% of the Earth's atmosphere). Although N_2O reduction is generally associated to denitrifying organisms, many N_2O reducers lack reductases other than N_2OR (i.e., nitrate-, nitrite-, or nitric oxide-reductase; Hallin et al. 2018). However, most, if not all, denitrifiers—and presumably N_2O reducers—are facultative aerobes, having the terminal oxidases necessary for O_2 respiration (van Spanning and Richardson 2007).

Based on what is known on the biochemistry of model organisms like *Paracoccus denitrificans*, N_2O and O_2 respiration presumably share the core of the ETC (Chen and Strous 2013), with electrons branching out to O_2 (via cytochrome oxidases), N_2O (via N_2OR), or other NO_x (in denitrifying N_2O reducers) depending on electron acceptor availability. It is a common notion that, when both N_2O and O_2 are available, N_2O reducers will consume O_2 preferentially over N_2O (and other N oxides; Shapleigh 2013). Even though N_2O is a stronger electron acceptor than O_2 in terms of thermodynamics, a number of authors have shown that N_2O respiration is energetically less efficient than aerobic respiration, resulting in lower biomass growth yields per substrate (Koike and Hattori 1975; Stouthamer et al. 1982; Beun et al. 2000). We cannot rule out the existence of a more energy-efficient N_2O reduction process (Conthe et al. 2018a), considering the broad phylogenetic diversity of N_2O reducers and our limited knowledge regarding non-denitrifying N_2O reducers in particular. However, given the growth yields reported in literature, it

Electronic supplementary material The online version of this article (https://doi.org/10.1007/s00253-018-9247-3) contains supplementary material, which is available to authorized users.

✉ Monica Conthe
M.conthecalvo-24@tudelft.nl

[1] Department of Biotechnology, Delft University of Technology, Van der Maasweg 9, 2629 HZ Delft, The Netherlands

Published online: 27 July 2018

would make evolutionary sense for microorganisms to favor aerobic respiration over the respiration of N compounds to optimize energy conservation in the cell. Intriguingly, the physical mechanism directing electrons to O_2 preferentially over other N compounds, when both electron acceptors are available, remains unclear.

Regulatory systems on a transcriptional or post-transcriptional level have been shown to shut down denitrification in the presence of oxygen in a variety of organisms (Zumft 1997). For instance, the NosZ protein of *Paracoccus denitrificans* and *Pseudomonas stutzeri* is inhibited by O_2 in vitro (Coyle et al. 1985; Alefounder and Ferguson 1982), which could be a form of allosteric regulation in vivo. It has also been proposed that N_2OR is—for reasons unknown—less competent than the cytochrome oxidases involved in respiration of O_2 in the "competition" for electrons in the ETC (Qu et al. 2015). Nevertheless, diverse studies have reported the occurrence of denitrification in the presence of O_2 (termed aerobic denitrification; Chen and Strous 2013 and references therein). Regarding N_2O reduction more specifically, a significant degree of N_2OR transcription and activity has been found under aerated conditions (Körner and Zumft 1989; Qu et al. 2015).

From a greenhouse gas mitigation point of view, it is interesting to study O_2 and N_2O mixotrophy—or the capability of microorganisms to simultaneously respire O_2 and N_2O—in order to understand how frequent oxic-anoxic shifts during nitrogen removal from wastewater, in space or time, may affect the N_2O-reducing capacity of activated sludge. WWTP design and operation vary greatly, but universal questions to address are, e.g., (a) if N_2OR activity can persist in aerated zones consuming nitrification-derived N_2O potentially minimizing greenhouse gas emissions or (b) if, on the contrary, N_2OR is relatively less active than the other NO_x reductases in the presence of O_2, leading to N_2O accumulation in the aerobic-anoxic transition zones.

We explored O_2 versus N_2O respiration in a continuous enrichment culture selected and grown with N_2O as the sole electron acceptor and fully characterized—in terms of stoichiometry and community composition—in a previous study (Conthe et al. 2018b). The culture had been found to be composed of a relatively simple microbial community dominated by *Dechlorobacter*-like *Betaproteobacteria*. In this study, operation of the chemostat was continued and the N_2O-limited steady-state conditions were intermittently interrupted to perform short-term batch experiments in situ, with varying concentrations of N_2O, O_2, or both N_2O and O_2 simultaneously, to determine (i) whether O_2 is, in fact, preferentially consumed over N_2O when both electron acceptors are available, (ii) under which O_2 concentrations (if any) N_2O consumption can take place, and (iii) to begin to unravel the mechanism governing the electron flow in the ETC to O_2 or N_2O.

Materials and methods

Chemostat operation

Following the work presented in Conthe et al. (2018b), a microbial enrichment using acetate as a carbon and energy source and exogenous N_2O as the sole electron acceptor was maintained under N_2O-limiting conditions in a continuous culture at 20 °C, pH 7, and a dilution rate of 0.026 ± 0.001 h^{-1}. The reactor set-up, operation, sampling, and medium composition are described in detail in Conthe et al. (2018b, c). One hundred percent pure N_2O gas diluted in Argon gas was fed to the chemostat at a total flow rate of 200 ml/min and the offgas from the reactor was recirculated at a rate of 700 ml/min, resulting in an incoming N_2O concentration of roughly 0.30%. The stability of the culture in terms of conversion rates and microbial community composition was monitored by regular sampling of the broth and biomass and via online monitoring of the acid (1 M HCl) dosing (a proxy for acetate consumption in the system) and offgas composition.

Batch experiments

The steady-state conditions of the culture were briefly interrupted on different operation days in order to perform batch experiments in situ and determine the maximum conversion rates of the enrichment under non-limiting conditions (Figure S1). The medium and effluent pumps were switched off and the gas supply rates of O_2 (from a bottle of pure O_2) and/or N_2O were modified to achieve different electron acceptor concentrations within the system in random steps. Two main types of batches were performed: (1) supplying a single electron acceptor—either N_2O or O_2—at different concentrations or (2) supplying N_2O and O_2 simultaneously, keeping the N_2O gas supply rate constant and varying that of O_2. Additionally, we performed a batch test in which a constant O_2 gas supply rate was maintained while varying that of N_2O as well as short batch tests with either NO_3^- or NO_2^- to assess the denitrifying capacity of the culture. Note that gas recirculation was maintained during the experiments, causing an apparent delay between the conversions in the chemostat and the offgas concentration values measured. To avoid acetate depletion, a concentrated solution of sodium acetate was added to the broth at the start of the experiments and the 1 M HCl solution used for pH control during continuous operation was replaced by 1 M acetic acid for the duration of the experiment. For the batch tests with NO_3^- and NO_2^-, these compounds were supplied as 1 M KNO_3 or 1 M KNO_2.

Analytical procedures

Samples from the reactor for analysis of acetate and NH_4^+ were immediately filtered after sampling (0.45-μm pore size

poly-vinylidene difluoride membrane, Merck Millipore, Carrigtohill, Ireland). Acetate was measured with a Chrompack CP 9001 gas chromatograph (Chrompack, Middelburg, The Netherlands) equipped with an HP Innowax column (Agilent Technologies, Santa Clara, CA, USA) and a flame ionization detector. Ammonium, NO_3^-, and NO_2^- concentrations were determined spectrophotometrically using cuvette test kits (Hach Lange, Düsseldorf, Germany). For the estimation of biomass concentration, the volatile suspended solids (VSS) concentration was determined by centrifuging 0.2 L of the enrichment, drying the pellet overnight at 105 °C, and then burning the pellet at 550 °C for 2 h to determine the ash content. Additionally, the optical density of the culture (at a wavelength of 660; OD_{660}) was monitored. Concentrations of N_2O, N_2 and CO_2, Argon, and O_2 in the headspace of the reactor were measured online via mass spectrometry (Prima BT, Thermo Scientific). The dissolved O_2 concentration in the broth during the batch tests with O_2 was measured with two types of oxygen sensors: a Clark electrode calibrated in the range of 0–20.8% and an optical oxygen probe calibrated in range 0–2% (Presens, Regensburg, Germany).

Calculations

Elemental and electron balances during steady state were set up as described in Conthe et al. (2018a, b, c). During the batch tests, the conversion rates (r, in mol h^{-1}) for O_2 and N_2O were calculated from the measured ingoing and outgoing gas composition and the argon supply rate (see Figures S2–S6 and Tables S2–S6 for details). The average biomass concentration value for each experimental step was derived from the ammonium uptake rates (see for example Figure S4b) and used to calculate the corresponding biomass specific rates (q, in mol $CmolX^{-1}$ h^{-1}). A standard and constant biomass composition of $CH_{1.8}O_{0.5}N_{0.2}$ (Roels 1980). The qO_2 and qN_2O obtained for each step were plotted against the corresponding concentration of dissolved O_2 or N_2O in the broth in order to determine the q_{max} and K_s of the enrichment for O_2 and N_2O. The concentration of dissolved O_2 was obtained experimentally with the DO probes while the concentration of dissolved N_2O was estimated given a k_La_{N2O} of 180 h^{-1}—obtained by scaling the experimentally derived k_La_{O2} (Janssen and Warmoeskerken 1987) and deriving the corresponding K_La_{broth} and $K_La_{headspace}$ assuming a t_{broth} of 6 s (1800 and 50 h^{-1}, respectively). A Monod model fitting the results was obtained by minimizing the sum of squared errors using the Microsoft Excel software.

The thermodynamic efficiency of metabolic growth using acetate as an electron donor and O_2, N_2O, or NO_3^- as an electron acceptor can be interpreted by the Gibbs free energy (ΔG01) dissipated per C mole of biomass growth or per electron-equivalent used for respiration. These values were calculated based on Kleerebezem and van Loosdrecht (2010) and using the thermodynamic values found in Thauer et al. (1977)—please refer to Table S7 for more details.

DNA extraction and 454 amplicon sequencing of 16S rRNA gene

The taxa-based community composition of the enriched culture during the period of operation presented in this study was determined by 454 amplicon sequencing of the 16S rRNA gene following the procedure described in Conthe et al. (2018a, b, c) and the sequences are available at NCBI under BioProject accession number PRJNA413885.

Results

Continuous operation and microbial community composition of the N_2O-reducing enrichment

A culture enriched from activated sludge using acetate as a carbon source and electron donor and exogenous N_2O as the sole electron acceptor was studied for a total period of 155 days (> 100 volume changes) in a chemostat under electron acceptor (N_2O) limiting conditions (Figure S1). The start-

Table 1 Average biomass-specific conversion rates during steady state and the batch experiments

	Compound biomass specific conversion rates (mmol/$mmol_X$ h^{-1})			
	$q_{N2O\text{-}N}$	$q_{NO3\text{-}N}$ or $q_{NO2\text{-}N}$	$q_{N2\text{-}N}$	$q_{Acetate\text{-}C}$
Steady state	− 0.033 ± 0.001[b]		0.034 ± 0.001[b]	− 0.017 ± 0.001[b]
N_2O batch	− 0.131 ± 0.004[b]		0.126 ± 0.008[b]	− 0.067 ± 0.009[c]
NO_3^- batch		− 0.007 ± 0.000[c]	0.004 ± 0.000[c]	− 0.003 ± 0.000[c]
$N_2O + NO_2^-$ batch[a]	− 0.033 ± 0.000[c]		0.042 ± 0.000[c]	

[a] N_2O gas supply was kept on during addition of 1 mM KNO_2^-

[b] Standard deviation calculated from at least three independent measurements

[c] Standard deviation calculated by LINEST least squares method

Table 2 Experimentally determined biomass yields per mole of electron donor or per mole of electron equivalents respired during growth with N_2O, NO_3^-, and O_2 as an electron acceptor and corresponding Gibbs free energy dissipation values based on these yields

	Parameter	Units	Growth on electron acceptor		
			N_2O[a]	NO_3^-[b]	O_2[c]
Y_{XS}	Biomass yield on acetate	$Cmol_X/Cmol_{Ac^-}$	0.36 ± 0.03	0.38	0.45
Y_{Xe}	Biomass yield on e^- transported in catabolic process	$Cmol_X/mol_{e^-}$	0.16 ± 0.01	0.15	0.19
$\Delta G^{01}{}_{MET}$	Metabolic energy change per mole donor[d]	$kJ/Cmol_X$	− 1078	− 620	− 479
$\Delta G^{01}{}_{e\ CAT}$	Metabolic energy change per electron transferred in catabolism	kJ/mol_{e^-}	− 159	− 96	− 101

[a] Steady state data, this study

[b] Steady state data—no siginificant accumulation of intermediates (Conthe et al.; data unpublished)

[c] Batch experiment data in N_2O reducing enrichment, this study

up and characterization of the enrichment during the first 70 days of operation, in terms of conversion rates, stoichiometry, and microbial community composition, are described in Conthe et al. (2018b). During the subsequent period reported here, the conversion rates and corresponding biomass yields remained consistent with the previous period, characterized by steady-state growth on acetate oxidation coupled to N_2O reduction to N_2 (Tables 1 and 2). Furthermore, 454 amplicon sequencing of the 16S rRNA gene of the microbial community confirmed the continued prevalence of a *Dechlorobacter*-like OTU (Figure S1), transiently co-occurring (around day 100) with two other closely related OTUs classified as *Azonexus* and uncultured *Rhodocyclaceae*.

O_2 vs. N_2O batch tests: affinity and yields

Batch experiments with varying supply rates of either N_2O or O_2 were performed on days 106 and 132, respectively (Fig. 1). The maximum biomass specific conversion rates of N_2O (q^{max}_{N2O}) and acetate were identified by increasing the N_2O supply rate to non-limiting conditions. The q^{max}_{N2O} values

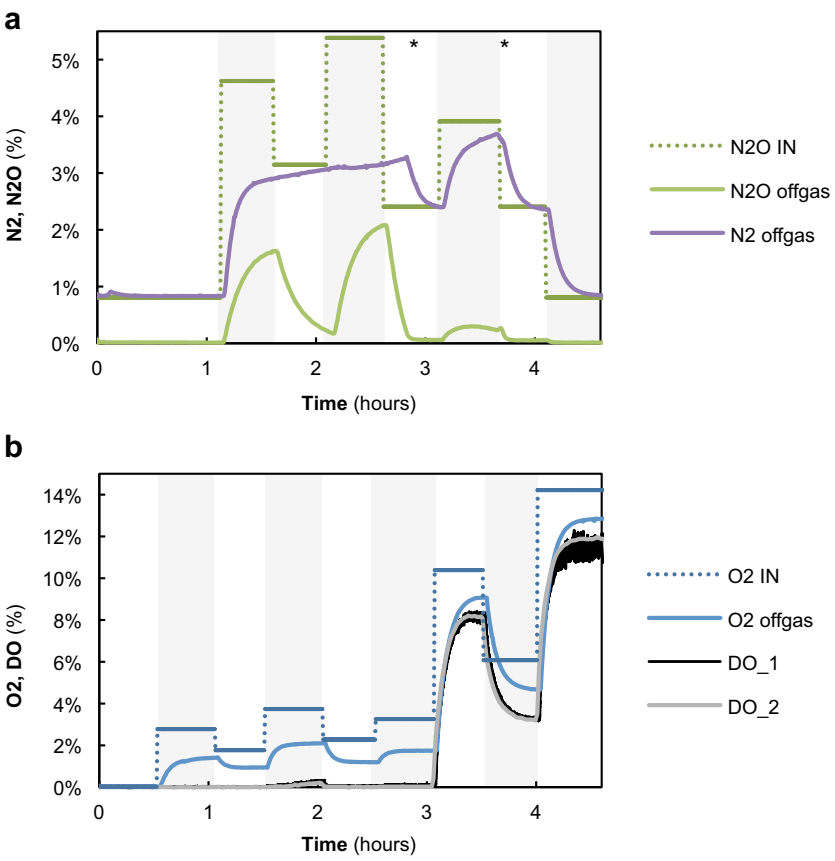

Fig. 1 Offgas data from the batch experiments with varying concentrations of **a** N_2O; day 106, **b** and O_2; day 132. For the experiment with O_2, the dissolved oxygen concentration (DO) was measured both with a Clark electrode (DO_1) and an optical sensor (DO_2). The affinity of the culture for N_2O and O_2 was determined from these experiments (see Fig. 5). The asterisk mark time points at which acetate had been depleted and was added to the culture

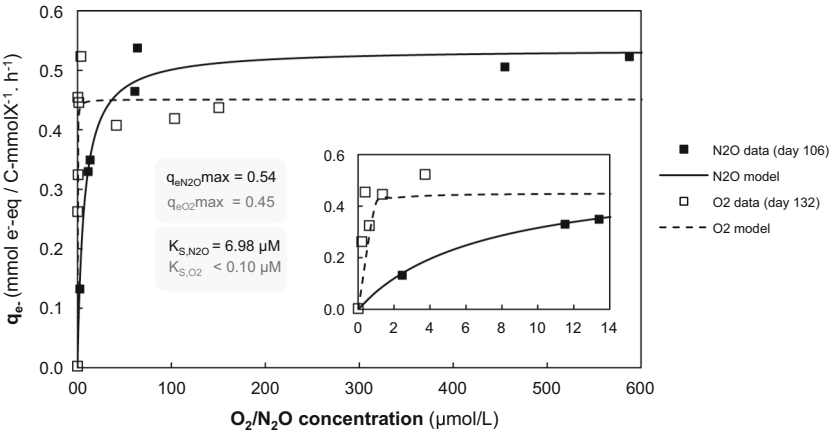

Fig. 2 Biomass specific transfer rates of electron equivalents (q_{e^-}) as a function of the electron acceptor concentration (either N_2O, in black, or O_2, in gray), along with the fitting Monod model (with the corresponding $q_{e^-}^{max}$ and K_s parameters). The inset is an enlargement of the graph at low O_2/N_2O concentrations. The rates presented were obtained from the experiments shown in Fig. 2

identified were roughly fourfold higher than the actual biomass specific conversion rates during steady state (Table 1). When exposed to varying concentrations of O_2, the culture was able to switch to aerobic respiration in the order of seconds. The maximum O_2 reducing capacity (q_{O2}^{max}) was comparable to N_2O respiration when expressed per mole electron accepted. NO_3^- and NO_2^- reducing capacities were much lower compared to N_2O or O_2 (< 15% of the maximum N_2O or O_2 reduction rate; Table 1).

Plotting the biomass-specific electron transfer rate (qe^-) at different dissolved O_2 (DO) or N_2O concentrations, we could determine the apparent K_s for O_2 or N_2O by fitting a Monod model to the data (Fig. 2). Given the confidence intervals, the absolute value for this parameter could not be identified accurately, but the results demonstrate clearly that the K_s value for O_2 is 1 or 2 orders of magnitude smaller compared to K_s-N_2O. The maximum biomass-specific conversion rate of O_2 (q_{O2}^{max}) was roughly two times lower than that of N_2O (q_{N2O}^{max}) per mole of electron acceptor but the conversion rates expressed as electron equivalents (q_e^{max}) were comparable for both processes, since double the electrons are taken up during the reduction of O_2 to H_2O compared to N_2O to N_2.

The biomass yields per mole of electron donor (determined from the steady-state growth on N_2O in the chemostat, and from the batch experiments with O_2 as the sole electron acceptor) are presented in Table 2.

Simultaneous O_2 and N_2O batch tests

Batch experiments with excess N_2O and varying concentrations of O_2, supplied simultaneously, were performed on days 110 and 155 (Figs. 3 and 4). The maximum electron transfer rate (q_e^{max})—combining the electron transfer capacities of N_2O and O_2—summed up to a value comparable with the

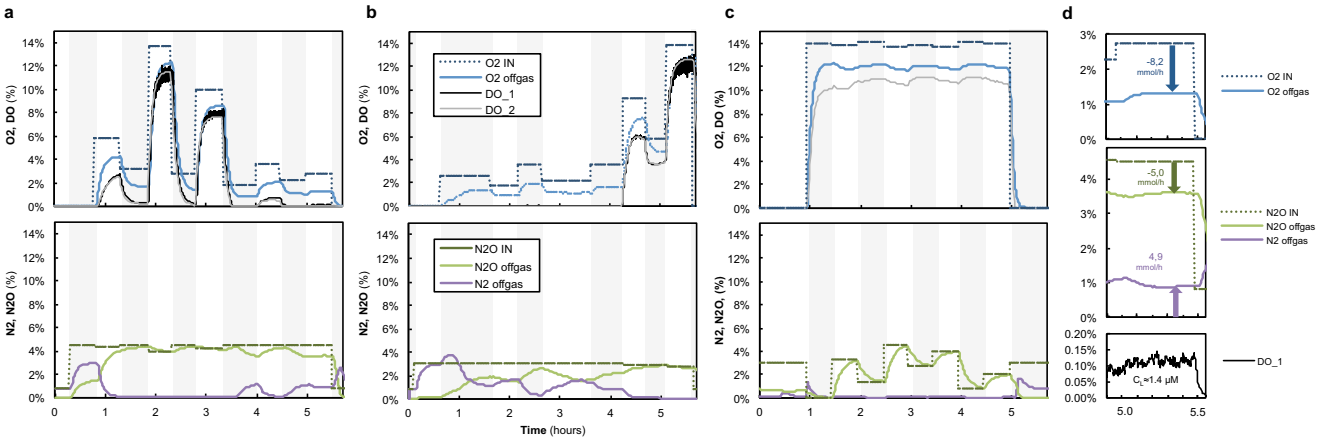

Fig. 3 Offgas data from the batch experiments with excess N_2O and varying concentrations of O_2 on **a** day 125 and **b** day 155. The dissolved oxygen concentration (DO) was measured both with a Clark electrode (DO_1) and an optical sensor (DO_2). The biomass specific electron transfer rates to either N_2O or O_2 during these experiments are shown in Fig. 4. The asterisk marking the last two steps of the batch experiment on day 155 indicates the culture ran out of NH_4^+ for growth, and thus the rates during these steps was not considered. **c** Offgas data of batch experiment with excess O_2 and varying concentrations of N_2O on day 113. Detailed data from these experiments can be found in the Supplementary Materiasl—Tables xxx–xxx and Figures xxx to xxx. **d** Detailed view of one of the steps from the batch experiment depicted in (**a**) showing the simultaneous consumption of O_2 and N_2O, and subsequent production of N_2

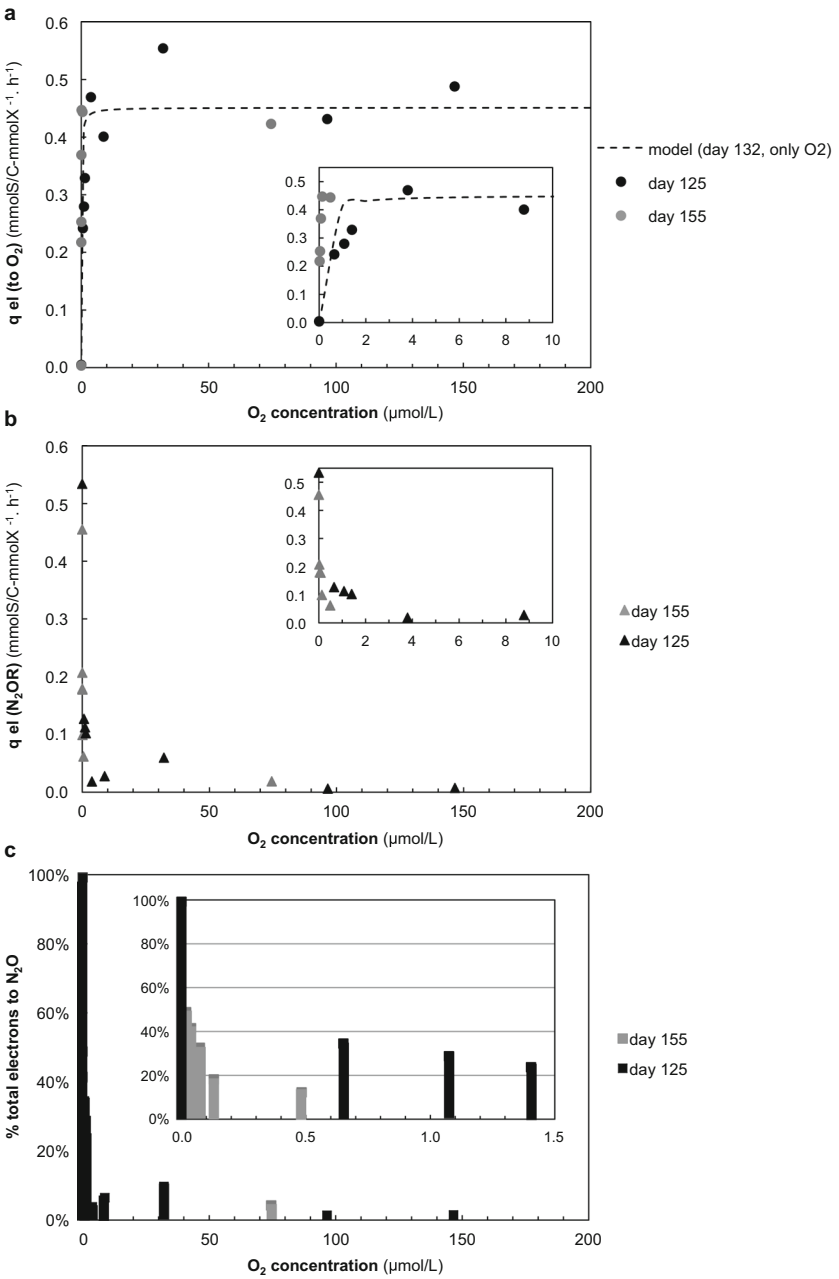

Fig. 4 Biomass specific transfers rate of electron equivalents (q_{e^-}) (**a**) to O_2 and **b** N_2O and **c** percentage of total electrons being shuttled to N_2O vs. O_2 at varying O_2 concentrations during the batch tests on day 125 (in black) and day 155 (in gray). The Monod model of O_2 consumption in the absence of N_2O (shown in Fig. 3) is included in (**a**) for comparison. The inset in (**c**) is an enlargement of the graph at low O_2 concentrations

q_e^{max} found during the N_2O- or O_2-only experiments. N_2O reduction to N_2 co-occurred with aerobic respiration only at relatively low concentrations of O_2 (Fig. 3d). The experiments performed on days 110 and 155 differed regarding the O_2 concentration range at which N_2O reduction could co-occur (roughly < 4 and < 1.5 μM O_2 on days 110 and 155, respectively) but, nevertheless, N_2O reduction in the presence of O_2 contributed to no more than a small fraction of the total electron acceptor capacity (generally < 20% of qe¯tot; Fig. 4). An additional batch experiment on day 113, with a constant supply of O_2 and a varying supply of N_2O, also showed that N_2O reduction was undetectable in the presence of relatively high concentrations of O_2 (≈5 μM; Fig. 3c).

Discussion

Aerobic respiration was distinctly favored over N_2O respiration in the enrichment despite the fact that the culture had been operated for an extensive number of generations with N_2O as only electron acceptor. Upon a sudden change in supply from N_2O to O_2, the culture readily switched to O_2 respiration and, when both electron acceptors were available, N_2O reduction was only observed at relatively low concentrations of O_2 (< 4 μM = 0.13 mg O_2/L). Under conditions of electron acceptor excess (N_2O and/or O_2), growth in the system was likely limited by the electron supply rate to the electron transport chain (see Fig. 5) and not by the capacity of N_2OR or O_2 reductases.

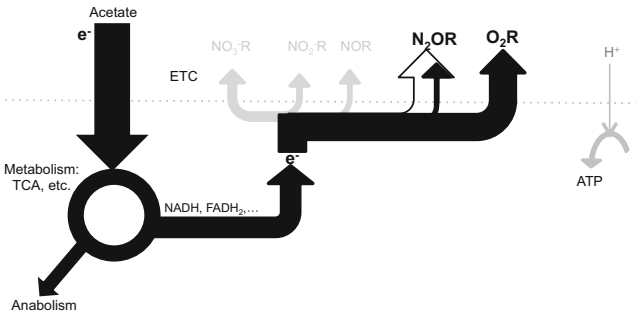

Fig. 5 Simplified representation of the proportional distribution of electrons (e^-) in the electron transport chain (ETC) during batch tests with only N_2O (open arrow) versus batch tests with the simultaneous addition of O_2 and N_2O (black arrows) showing that there is a preferential shuttling of electrons to O_2R than to N_2OR. This simplified schematic is based on the assumptions that (i) both enzymes share a common electron pool (/quinone pool) and (ii) that all cells have a similar electron distribution among terminal reductases (whereas it would be possible for the majority of cells to switch fully to aerobic respiration, and a small fraction to continue respiring N_2O)

This was inferred from the fact that the maximum electron acceptor capacity of the culture was comparable for N_2O and O_2 respiration (i.e., $q^{max}_{e^-N2O} \approx q^{max}_{e^-O2}$), and could be due to kinetic limitations in acetate uptake, acetate oxidation in the citric acid cycle, or in some shared component of the ETC itself.

The overall electron transfer capacity during the simultaneous respiration of N_2O and O_2 (i.e., $q^{max}_{e^-TOT}$) was comparable to $q^{max}_{e^-N2O}$ or $q^{max}_{e^-O22}$. This suggests that "aerobic N_2O respiration" (by analogy to aerobic denitrification) generally occurs if the electron supply rate to the ETC exceeds the electron accepting capacity of the O_2 reductases. In other words, N_2O respiration complements aerobic respiration primarily when O_2 is limiting. Nonetheless, our results indicate that, under O_2-limiting conditions, N_2O reducers can use O_2 and N_2O mixotrophically as proposed by Chen and Strous 2013 (Fig. 5). We cannot exclude heterogeneity in electron acceptor use within the population in our bioreactor leading for example to most of the culture respiring O_2 and a side population reducing N_2O. Under the microscope, we did not observe formation of aggregates or biofilms which could create anoxic niches in spite of the O_2 supply (data not shown), yet oxygen gradients and anoxic microzones could still form around suspended cells if O_2 diffusion rate is slower than the respiration rate. Nevertheless, with the strong sparging and mixing conditions imposed on the culture, we would expect that most cells would be exposed to comparable environmental conditions.

The K_s values of the enrichment culture were in the same range as the K_m values reported for purified N_2OR and different O_2 reductases in literature, i.e., in the μM range for N_2O and nM range for O_2 (Pouvreau et al. 2008 and references therein, Yoon et al. 2016). The relatively high $K_{S,N2O}$ (two orders of magnitude higher than for O_2) is noteworthy in a culture presumably well-adapted to N_2O-limiting conditions. Also the observation that, even after a prolonged absence of O_2 in the environment, the cellular machinery specific for aerobic respiration (i.e., cytochrome oxidases) was constitutively present (in contrast to NO_3^- and NO_2^- reductases). According to these results, the preferential use of O_2 over N_2O in natural systems could be attributed to a difference in affinity (μmax/K_s) for O_2 and N_2O.

With regard to efficiency of N_2O respiration versus O_2 respiration, our chemostat enrichment cultures corroborate studies in literature (Koike and Hattori 1975; Stouthamer et al. 1982; Beun et al. 2000) and predictions based on our knowledge of the ETC in model denitrifiers (Chen and Strous 2013): with biomass yields per mole of acetate during growth with N_2O (or NO_3) roughly 1/3 lower than yields during O_2 respiration (Table 2). The relatively low growth yields on N_2O imply that N_2O reduction to N_2 is, thermodynamically, a very inefficient process with high energy dissipation. Thus, ensuring the maximization of energy conservation during microbial growth may be the evolutionary driver behind the preferential flow of electrons to O_2 over N_2O.

We cannot provide a conclusive answer regarding which cellular mechanism governs the preferential use of O_2 in the presence of excess N_2O observed. However, the instantaneous switch from N_2O to O_2 respiration suggests that the preference for O_2 over N_2O is regulated at the metabolome level and is independent from transcriptional regulation, e.g., by control of enzyme activity, like allosteric inhibition of N_2OR, or simply a higher affinity of O_2 reductases for the electrons coming from a common quinone pool.

Translated to the environmental conditions in a WWT plant, the results from this study suggest that oxic-anoxic transitions are unlikely to result in N_2O emissions associated to denitrification as a result of N_2OR inhibition by O_2 since the enrichment culture readily switched back and forth between O_2 and N_2O respiration. This implies that (a) either N_2OR is not directly inhibited by O_2 in vivo or (b) inhibition is readily reversible once O_2 is depleted.

On the other hand, the fact that aerobic respiration is so strongly favored over N_2O respiration would make it a challenge to exploit the N_2O sink capacity of activated sludge in the aerated/nitrification zones of WWT plants. The range in which significant N_2O consumption co-occurred with O_2 consumption in our experiments was narrow: roughly up to 1.5–4 μM O_2, i.e., 0.05–0.13 mg O_2/L, presumably below common DO values in the aerated tanks of WWTP (Tchobanoglous and Burton 2002). The very high affinity for oxygen minimizes the range of dissolved oxygen concentrations in which O_2 and N_2O respiration could occur in parallel. However, a beneficial difference in full-scale systems compared to our enrichment, in terms of avoiding N_2O accumulation, may be that mass transfer limitation induced oxygen limitation within the activated sludge flocs provide anoxic zones, prone to N_2O reduction, even when O_2 is present in the bulk liquid (Picioreanu et al. 2016). This, together with the fact that N_2O is much more soluble than O_2, could perhaps be exploited to enhance the N_2O sink capacity of activated sludge.

Acknowledgements The authors would like to thank Gijs Kuenen for his comments on the manuscript and Mitchell Geleijnse and Ben Abbas for their great help with the molecular analysis of microbial community composition.

Funding This work was funded by the European Commission (Marie Curie ITN NORA, FP7-316472).

Compliance with ethical standards

Conflict of interest The authors declare that they have no conflict of interest.

Ethical approval This article does not contain any studies with human participants or animals performed by any of the authors.

References

Alefounder PR, Ferguson SJ (1982) Electron transport-linked nitrous oxide synthesis and reduction by Paracoccusdenitrificans monitored with an electrode. Biochem Biophys Res Commun 104 (3):1149–1155

Beun JJ, Verhoef EV, Van Loosdrecht MCM, Heijnen JJ (2000) Stoichiometry and kinetics of poly-β-hydroxybutyrate metabolism under denitrifying conditions in activated sludge cultures. Biotechnol Bioeng 68:496–507

Chen J, Strous M (2013) Denitrification and aerobic respiration, hybrid electron transport chains and co-evolution. Biochim Biophys Acta Bioenerg 1827:136–144

Conthe M, Kuenen JG, Kleerebezem R, van Loosdrecht MCM (2018a) Exploring microbial N_2O reduction: a continuous enrichment in nitrogen free medium. Environ Microbiol Rep 10:102–107. https://doi.org/10.1111/1758-2229.12615

Conthe M, Wittorf L, Kuenen JG, Kleerebezem R, Hallin S, van Loosdrecht MCM (2018b) Growth yield and selection of nosZ clade II-types in a continuous enrichment culture of N_2O respiring bacteria. Environ Microbiol Rep 10:239–244. https://doi.org/10.1111/1758-2229.12630

Conthe M, Wittorf L, Kuenen JG, Kleerebezem R, van Loosdrecht MCM, Hallin S (2018c) Life on N_2O: deciphering the ecophysiology of N_2O respiring bacterial communities in a continuous culture. ISME J. https://doi.org/10.1038/s41396-018-0063-7

Coyle CL, Zumft WG, Kroneck PMH, Körner H, Jakob W (1985) Nitrous oxide reductase from denitrifying: *Pseudomonas perfectomarina* purification and properties of a novel multicopper enzyme. Eur J Biochem 153:459–467

Hallin S, Philippot L, Löffler FE, Sanford RA, Jones CM (2018) Genomics and ecology of novel N_2O-reducing microorganisms. Trends Microbiol 26:43–55

Janssen LPBM, Warmoeskerken MMCG (2006) Transport phenomena data companion, Third edit edn. VSSD, Delft

Kleerebezem R, van Loosdrecht MCM (2010) A generalized method for thermodynamic state analysis of environmental systems. Crit Rev Env Sci Technol 40(1):1–54

Koike I, Hattori A (1975) Energy yield of denitrification: an estimate from growth yield in continuous cultures of *Pseudomonas denitrificans* under nitrate-, nitrite- and oxide-limited conditions. J Gen Microbiol 88:11–19

Körner H, Zumft WG (1989) Expression of denitrification enzymes in response to the dissolved oxygen level and respiratory substrate in continuous culture of *Pseudomonas stutzeri*. Appl Environ Microbiol 55:1670–1676

Picioreanu C, Erez JP, Van Loosdrecht MCM (2016) Impact of cell cluster size on apparent half-saturation coefficients for oxygen in nitrifying sludge and biofilms. https://doi.org/10.1016/j.watres.2016.10.017

Pouvreau LAM, Strampraad MJF, Van Berloo S, Kattenberg JH, de Vries S (2008) NO, N_2O, and O_2 reaction kinetics: scope and limitations of the Clark electrode. Methods Enzymol 436:97–112

Qu Z, Bakken LR, Molstad L, Frostegård Å, Bergaust L (2015) Transcriptional and metabolic regulation of denitrification in *Paracoccus denitrificans* allows low but significant activity of nitrous oxide reductase under oxic conditions. Environ Microbiol 18:2951–2963. https://doi.org/10.1111/1462-2920.13128

Roels JA (1980) Simple model for the energetics of growth on substrates with different degrees of reduction. Biotechnol Bioeng 22:33–53

Shapleigh JP (2013) Denitrifying Prokaryotes. In: Rosenberg E, DeLong EF, Lory S, Stackebrandt E, Thompson F (eds) The prokaryotes: prokaryotic physiology and biochemistry. Springer Berlin Heidelberg, Berlin, pp 405–425

Stouthamer AH, Boogerd FC, van Verseveld HW (1982) The bioenergetics of denitrification. Antonie Van Leeuwenhoek 48:545–553

Thauer RK, Jungermann K, Decker K (1977) Energy conservation in chemotrophic anaerobic bacteria. Bacteriol Rev 41:100–180

Tchobanoglous G, Burton F, Stensel HD (2006) Wastewater engineering—treatment and reuse. McGraw-Hill, New York

Thomson AJ, Giannopoulos G, Pretty J, Baggs EM, Richardson DJ (2012) Biological sources and sinks of nitrous oxide and strategies to mitigate emissions. Philos Trans R Soc Lond Ser B Biol Sci 367:1157–1168

van Spanning RJM, Richardson DJ, Ferguson SJ (2007) Introduction to the biochemistry and molecular biology of Denitrification. Biology of the Nitrogen Cycle 3–20. https://doi.org/10.1016/B978-044452857-5.50002-3

Yoon S, Nissen S, Park D, Sanford RA, Löffler FE (2016) Nitrous oxide reduction kinetics distinguish bacteria harboring clade I NosZ from those harboring clade II NosZ. Appl Environ Microbiol 82:3793–3800

Zumft WG (1997) Cell biology and molecular basis of cell biology and molecular basis of Denitrification. Microbiology 61(4):533